F. Toffol, L. Marchetti, A. De Gaspari, J.V. Chardí Espí, L. Riccobene, F. Fonte, S. Ricci, P. Mantegazza
Design and Experimental Validation of Gust Load Alleviation Systems Based on Static Output Feedback
in: AIAA Scitech 2022 Forum, AIAA, 2022, ISBN: 9781624106316, p. 1-18, AIAA 2022-0441
[AIAA Scitech 2022 Forum, San Diego, CA, USA & Virtual Conference, 3-7 Jan. 2022]
doi:10.2514/6.2022-0441

Design and Experimental Validation of Gust Load Alleviation Systems based on Static Output Feedback

F.Toffol[1], L.Marchetti[2], A.De Gaspari[3], J. V. Chardí Espí[4], L.Riccobene[5], F. Fonte[6], S. Ricci[7] and P.Mantegazza[8]

Politecnico di Milano, Department of Aerospace Science and Technology, 20156 Milano, Italy

Abstract

The paper summarizes the activity performed in the framework of the EU funded project CS2-AIRGREEN2 aiming at the development and testing of Gust Load Alleviation technologies applied to the so-called Green Regional Aircraft. An extended numerical activity carried out on the reference aircraft established the due knowledge to start designing the experimental model and the systems for the final wind tunnel validation. The wind tunnel model is representative of the half aircraft having a geometrical scale equal to 1:6. The wing is fully aeroelastic, and the model is installed on a dedicated system, named Weight Augmentation System (WAS), allowing for pitch and plunge free motions. The paper describes in the details the wind tunnel model, the adopted controllers and reports the relevant results collected during the experimental campaign carried out at Large POLIMI's wind tunnel.

I. Introduction

The need for more efficient aircraft able to meet the new challenging emissions requirements force the researchers to look for more advanced aircraft configurations, based on more efficient aerodynamics and structures together with more sophisticated flight control systems. The aircraft industry has to be able to deliver new significantly greener aircraft with a substantial reduction of fuel consumption, emissions, and perceived noise levels [1-3]. In this huge effort impacting the entire aeronautical community aiming at matching the stringent requirements of environmental impact defined in Europe and the US, many are the technologies under investigation. Among them, the extended adoption of active controls in general, and specifically the maneuver and gust loads alleviation technologies (MLA/GLA), are considered among the most promising. Despite they for sure are not new, when they are combined with other new technologies such as advanced composites, enhanced actuation systems, unconventional control surfaces and structural configurations, the synergetic effect could produce significantly improved performances.

Most of the applications of active controllers for MLA and GLA purposes are based on the use of standard control surfaces of the aircraft, usually ailerons and elevator. There are however some exceptions where the controllers had the possibility to use dedicated control surfaces specifically designed and installed for load alleviation. One particular situation where additional control surfaces are used occurs when fuselage modes need to be controlled, as in the case of the LAMS system [4] or the fuselage mode suppression system mounted on the B-1 Lancer aircraft [5]. There are also examples of aircraft equipped with control surfaces dedicated to gust alleviation, like the GLAS surface mounted on the B-23 and the Direct Lift Control (DLC) flaps mounted on the ATTAS aircraft [7]. Dedicated control surfaces were also studied in wind tunnel models, in [8] a trailing edge surface was used for load alleviation but resulted not very effective, different configurations of wing tip surfaces were applied to the EuRAM model [9] and a series of numerical studies [10], [11] provide an example of the good performances of the devices. A canard was used in the wind tunnel test described in [12] complementing the use of a split aileron, while a set of four trailing edge flaps is under investigation by NASA in the so-called VCCTEF [13] with the purpose of giving to the controller the possibility to alleviate the gust loads without affecting the capability to maneuver the aircraft.

1 PostDoc Graduate student, Politecnico di Milano
2 PhD Candidate, Politecnico di Milano
3Assistant Professor, Politecnico di Milano
4 Graduate student Politecnico di Milano
5Wind tunnel test engineer, Politecnico di Milano
6Formerly PostDoc Researcher, Politecnico di Milano, now analyst at Leonardo Helicopters.
7Professor, AIAA senior member, Politecnico di Milano
8Professor, Politecnico di Milano

A different approach to the MLA and GLA purpose can be based on providing an aircraft with additional aerodynamic surfaces placed on the wing tip equipped with an actively controlled surface. It is well known that increasing the span of an aircraft offers the advantage of increasing the aspect ratio so improving its aerodynamic efficiency, but usually at the expense of an increase in loads. The loads increase can be mitigated by designing the chord and twist distribution of the wing in order to obtain the desired value of wing root bending moment [14, 15]. However, in many applications, the wing tip extension needs to be applied as a retrofit to an existing aircraft, without the possibility to redesign the wing to limit the load increase. Withcomb showed that winglets are more suitable than wing tip for increasing aerodynamic efficiency [16]. However, in an optimization study performed in [17], he further analyzed the differences between winglets and wing tip and showed how the optimal solution can depend on the maximum lift coefficient required, with the winglet performing better when maneuvering conditions with high lift coefficients are included in the analysis. A possible solution to overcome the limitations in the performances of the wing tip extensions is to provide them with some active or passive alleviation capability. In the framework of the development of Gust Load Alleviation Technologies, the paper describes the design, development, and test of an innovative wingtip named IWT, that can be used alone or in combination with the primary controls, such as aileron and elevator to enhance the GLA capabilities.

II. The AIRGREEN2 Project

The AIRGREEN2 research project was conceived within the general framework of Clean Sky 2 (CS2) Program, responding to a specific call (JTI-CS2-CPW1-REG01-02). In line with the agenda of ACARE [3] and according to the current trend of the aerospace market, CS2 pursues:

- an efficient environmentally friendly transport
- a more and more safe and seamless mobility
- a more competitive aerospace European sector, promoting synergic relationships among the different actors (industries, small and medium enterprises, research centers, universities)

CS2 foresees three main Innovative Aircraft Demonstrator Platforms (IADPs), namely, fast rotorcraft, passenger and regional aircraft. For each of them, a specific development plan is envisaged, involving three different families of Integrated Technology Demonstrators (ITD), that is to say, airframe, engine, and systems (avionics and various equipment). From the technology readiness level (TRL) point of view, the Program aims at maturing already established technologies (TRL greater than 3) and demonstrating them in relevant environments, ranging from wind tunnel up to flight demo (arriving at least at a TRL of 5). AIRGREEN2 Project (2015-2022) finds its place within the regional aircraft platform IADP, led by Leonardo Aircraft Division.

The structure of the Project is based on three main top-level targets:

- The enhancement of the life cycle features, mainly involving the wing box structure and dealing with the synergic use of design and manufacture processes together with advanced strategies of structural health monitoring and repair
- The improvement of the aerodynamic performance, relying upon the following main technologies: natural laminar flow (wing optimized geometry, for aerodynamic drag abatement), riblet integrated skin (for better control the flow at the boundary layer level) and the high lift generation and climb control
- The assessment of the load control and alleviation architecture, involving conventional and unconventional, additional control surfaces; the investigated strategies, operating also in maneuver and gust conditions, target even conflicting optimal distributions of loads, in terms of aerodynamic performance (climb and cruise) and of load reduction.

Department of Aerospace Science and Technology (DAER) of Politecnico di Milano (POLIMI) in Italy, core partners of the AIRGREEN2 project, is in charge of coordinating all the activities related to the development and implementation of MLA/GLA technologies involving other partners such as Politecnico di Torino (POLITO), CIRA and UMBRA. They are based on both conventional control surfaces, such as the primary commands like aileron and elevator, as well as on dedicated non-conventional ones. Among them, a wing tip extension equipped with a movable control surface has been conceived, numerically tested on a reference full-scale aircraft, and validated with wind tunnel tests on an aeroelastic large-scale model. In 2022 a flight test campaign on a full-scale aircraft will be carried out at the conclusion of the research program.

The paper presents the activities carried out at DAER during the AIRGREEN project related to MLA/GLA technologies together with the full-scale simulation results as well the wind tunnel results on the scaled model.

III. The Reference Regional Aircraft

The Green Regional Aircraft, one of the six Clean Sky platforms introduced since the Clean Sky 1 Program, led by LEONARDO COMPANY-Aircraft Division, one of the ITD members, involved 32 European partners among engine manufacturers, system engineering companies, research centers, universities, small and medium enterprises.
The future green regional aircraft will meet demanding weight reduction, energy and aerodynamics efficiency, a high level of operative performance, in order to be compliant regards to pollutant emissions and noise generation levels. To achieve these so challenging results, the aircraft will be entirely revisited in all of its aspects.
The GRA structure is as follows:

- GRA1 - Low Weight Configuration (LWC)
- GRA2 - Low Noise Configuration (LNC)
- GRA3 - All Electric Aircraft (AEA)
- GRA4 - Mission & Trajectory Management (MTM)
- GRA5 - New Configuration (NC)

and reflects its transversal nature by being organized in 5 domains, that in turn interface with the other Cleansky platforms, such as Eco-Design (EDA for Airframe with LWC, EDS for System with AEA), System for Green Operation with AEA and MTM, and Sustainable and Green Engine (SAGE) with NC.
The research activity carried out by the AIRGREEN2 project as part of the Clean Sky 2 Program, the natural continuation of Clean Sky 1, involves the development of an advanced twin prop 90 pax regional aircraft called TP90, represented in the following Figure 1.

Figure 1: Pictorial view of TP90 aircraft.

IV. The Gust Loads Alleviation Controllers

Literature reports a lot of activities related to the design and implementation of maneuver and gust load alleviation technologies [18-32]. In the framework of the AIRGREEN2 project, different controllers for gust loads alleviation have been analyzed from different partners, but POLIMI mainly focused on the Static Output Feedback (SOF) [33]. The aero-servo-elastic system is modelled in with a State-Space representation where **x** is the state, **y** the available measures, **z** the performance, **u** the control input and **d** the external disturbance (e.g. gust).

$$\begin{cases} \dot{\boldsymbol{x}} == \boldsymbol{A}\boldsymbol{x} + \boldsymbol{B}_{\boldsymbol{u}}\boldsymbol{u} + \boldsymbol{B}_{\boldsymbol{d}}\boldsymbol{d} \\ \boldsymbol{y} = \boldsymbol{C}_{\boldsymbol{y}}\boldsymbol{x} + \boldsymbol{D}_{\boldsymbol{yu}}\boldsymbol{u} + \boldsymbol{D}_{\boldsymbol{yd}}\boldsymbol{d} \\ \boldsymbol{z} = \boldsymbol{C}_{\boldsymbol{z}}\boldsymbol{z} + \boldsymbol{D}_{\boldsymbol{zu}}\boldsymbol{u} + \boldsymbol{D}_{\boldsymbol{zd}}\boldsymbol{d} \end{cases}$$

The SOF arcitecture is based on the use of an algebraic relationship between the measurements $\boldsymbol{y} \in \Re^{ly}$ extracted from the system and the control input $\boldsymbol{u} \in \Re^{mu}$, defined by a gain matrix $\boldsymbol{G}$ such that $\boldsymbol{u} = \boldsymbol{G}\boldsymbol{y}$. The gain matrix is computed by the minimization of the $\mathfrak{H}_2$ norm of the closed-loop transfer function, relating some external disturbance to the performance output **z**, which can be expressed as a function of the gain matrix as

$$J(\boldsymbol{G}) = \frac{1}{2}\int_0^{\infty} [\mathbf{z}^{\mathbf{T}}\mathbf{W}_{\mathbf{zz}}\mathbf{z} + \mathbf{u}^{\mathbf{T}}\mathbf{W}_{\mathbf{uu}}\mathbf{u}]$$

(9) $\boldsymbol{W_{zz}}$ and $\boldsymbol{W_{uu}}$ are weighting matrices that are used to define the relative importance of the components of the control input and of the performance output. In the present work, the algorithm presented in [34] is used for the minimization of the cost function $J(\boldsymbol{G})$. The controller is based on the use of accelerometric measurements taken on the wing, as well as the rigid motion of the aircraft obtained from an Inertial Measurement Unit (IMU), the location of the sensors is shown in Figure 2. The torsional and bending moments are the main targets of the GLA controller, the pitch angle and rate are included in the cost function with a small weight in order to ensure adequate damping for the rigid motion of the aircraft. The evaluation of the closed-loop transfer function requires also the definition of the disturbances, which are taken to be the gust input and the noise on the measurements, with a shaping filter used to define the frequency content of the gust in order to reproduce that of a deterministic *1-cos* gust:

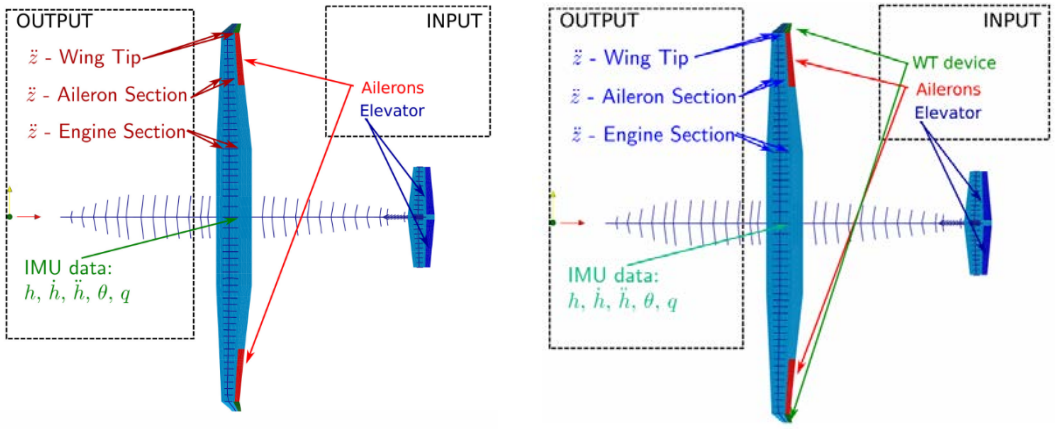

Figure 2: Different inputs and outputs configurations Root Bending Moment gust load reduction using SOF controller.

Different architectures of the controller have been investigated. In particular, the one based on the use of standard primary controls only, i.e. elevator and ailerons, and the one based on the full set of control surfaces, including the IWT, as well as the one based on IWT only, to be adopted in the case of retrofit on an already available aircraft. Figure 2 shows the different architecture of the inputs and outputs adopted. Figure 3 shows an example of the expected gust load alleviation capabilities obtained on the full aircraft using the different control architectures.

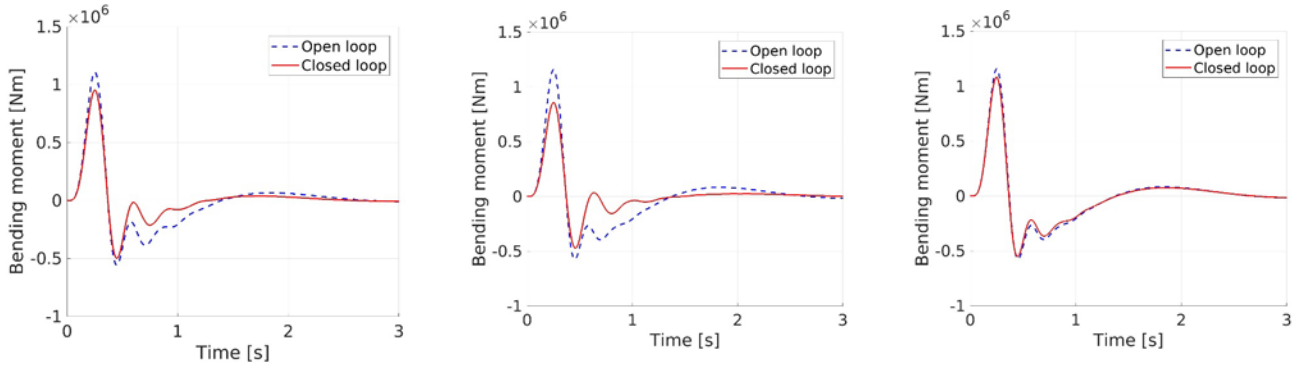

a) Aileron + Elevator b) Aileron + Elevator + IWT c) IWT only

Figure 3: Root Bending Moment gust load reduction using SOF controller.

The results mentioned above form the basis for the comparison of the performances with and without IWT and, most important, the target performances to be validated during the experimental campaign in the wind tunnel. The design procedure used for the definition of the SOF controller is replicable and the same cost function can be applied to different models, in this way there is a direct correlation between the closed-loop results obtained with the different configurations.

V. The Wind Tunnel Model WTT3

The wind tunnel model representative of the reference Regional Aircraft, name WTT3, has been designed as a half model with a fully aeroelastic wing capable of free plunge and pitch motions. The finalization of the model configuration implies the selection of the geometrical scale and the definition of the scaling method. Concerning the geometry scale, taking into account the maximum size available at the POLIMI's wind tunnel and the minimum model size requested by the call, the geometry scale has been frozen to 1:6.

Concerning the dynamic scaling strategy, the following considerations have to be introduced at first:

- The model is constrained at the floor and hence vertically mounted.
- Gravity will simply act in the direction of the wingspan and will not be reacted by the lift force
- When compared to deflections due to aerodynamic forces, the gravitational contribution will be insignificant
- The ratio of the elastic and weight force cannot be preserved. In our case, we can simply set the initial angle of attack to the expected lift coefficient and accept the resulting static deformation
- A different response for the rigid body dynamics would be expected for a free-free flying model where gravity appears in the dynamic equations

A. Aeroelastic Scaling

Traditionally the dynamically scaled models adopt a constant Froude number approach. This choice poses some practical problems. The most important one is that the time scale at the model level is increased by the square root of the geometry scale meaning that the phenomena at the model scale result accelerated. In the case of active control tests, it means that the bandwidth of the actuators requested for the scale models must be higher than the ones at full-scale level, making sometimes impossible to test the active controls for the difficulty to find miniaturized actuators with the requested bandwidth fitting the small space available in the models. For these reasons the iso-frequency scaling strategy has been adopted as the most suitable in this case, based on DAER experience acquired in a previous EU project named CS1-GLAMOUR [35]. With this scaling strategy, the frequency of the most relevant model mode shapes is equal to the corresponding ones of the full-scale reference aircraft. It must be pointed out that, due to the vertical position of the wing, and due to the presence of the Weight Augmentation System (WAS), which will be introduced later, it is possible to combine Froude and iso-frequency scaling strategies at the same time.

Given the maximum capability of the wind tunnel, compressibility is presumed to have no effect. One of the most evident limitations is imposed by the wind tunnel test section dimensions that defined the geometry scaling of 1:6 as the largest size of the half model reachable. If the characteristic dimensions are denoted with subscripts M and R for model and reference, respectively, it means:

$$L_M = \frac{L_R}{6}$$

By adopting the iso-frequency scaling, the ratio of model natural frequencies to reference eigenvalues is set to one. As a consequence, the natural frequencies of the wind tunnel model will be the same as the full-scale reference aircraft:

$$\omega_{o,M} = \omega_{0,R}$$

Note that imposing the natural frequencies of the reference on the wind tunnel model also fixes the time scaling $\lambda_t=1$, allowing to solve for the required freestream velocity scaling from the following:

$$V_{\infty,M} = \frac{V_{\infty,R}}{6}$$

Given that the scope of the test, not only the dynamics of the structure should be scaled, but also the unsteady aerodynamics should be equivalent between reference and model. To these matters, the reduced frequency ($k=\omega b/2V$) ratio becomes:

$$k_M = k_R$$

After simple manipulations (constant ratio between aerodynamic and elastic or inertial forces) it is easy to derive the scaling factors impacting the structural and mass properties of the model, such as:

$$EA_M = \frac{EA_R}{6^4}, EJ_M = \frac{EJ_R}{6^6}, GJ_M = \frac{GJ_R}{6^6}, M_M = \frac{M_R}{6^3}$$

As commonly happens, not all physical quantities can be scaled, preserving the already defined scaling factors. In particular, the speed of sound could not be preserved, leading to a drastic reduction in Mach compared to the reference conditions. Given that no transonic effects are predicted in the selected reference flight the results should be qualitatively similar. Also, the viscosity of the flow field during testing could not be tuned, leading to a reduction in Reynolds number Re compared to the reference. However, the flow regime was supposed acceptable. Last but not least, gravity appears in the non-dimensional equations of motion through the Froude number *Fr*. This non-dimensional parameter relates inertial to gravity effects. Hence, in principle, it was not possible to preserve it. Thoughtfully, the model is oriented in a nonconventional sense, with the wing rising vertically. This led to gravity not affecting the model in the traditional way. The Weight Augmentation System (WAS), described in one of the next sections, would feed a scaled virtual gravity, required to retrieve Froude unity.

B. The Wing Structure

The wing of the WTT3 model has been designed following the scaling factor introduced in the previous section. The component that was specifically designed to match the reference dynamics is the wing spar. This slender structural component stemmed from the wing root to the tip and would support all other components. Significant know-how was developed from previous experience at DAER where di different spar geometries have been investigated. Simpler spar designs have proven to be more cost-effective, driving the design philosophy in that direction. A hollow square section beam was selected as the base for the design. Its dimensions were bound by the space available within the scaled aerodynamic profiles. Adequately capturing the span varying stiffness distribution required the variation of the spar properties somehow. This was obtained by adding extra plates of aluminium to the original spar beam spanwise to match the reference stiffness properties. From the Reference Aircraft stick model, the equivalent mass and CoG of the engine were calculated. Structurally the entire nacelle was approximated by an equivalent arm once again realized by an aluminium beam considered rigid since no specific details about possible elastic or dynamic behaviour were available. A lump of lead was introduced at the free end of the tip of the beam to reproduce the engine mass. Finally, the wing aerodynamic shape was reproduced by seven aerodynamic sectors spanwise made by 3D printing in Winform material and connected to the main spar by means of a single bolt as to avoid adding extra stiffness to the spar (see Figure 4 and Figure 5).

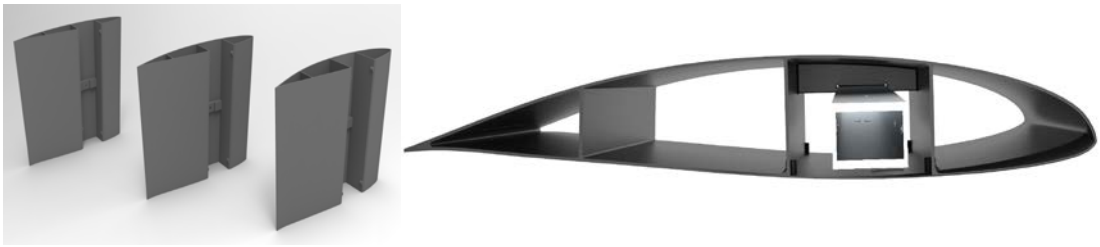

Figure 4: Aerodynamic sectors realized by 3D printing.

Figure 5: The final assembled wing with an internal view of the nacelle.

C. The Wing Actuation Systems

A concept with two hinge points, one at each extremum of the aileron, had already been successfully implemented in the past. An analogous mechanism was proposed here. From the wing root outwards, a first rib serves as an inner

hinge once the ball bearing installed but also as a support for the aileron servo actuator. This first rib is the one seen on the left-hand side of Figure 6 where it is possible to see how the entire mechanism fits within the wing internal space including the actuator without special issues. More complex is the installation of the IWT actuation. The solution was to realize a single machined rib to finalize the wing and to support the second hinge of the aileron, as well as the actuator and the IWT and its structure. The IWT is divided into two parts, upper and lower, connected together by bolts (see Figure 7). For both the control surfaces aileron and IWT, the RSF-5B by Harmonic Drive has been adopted, capable of high force and bandwidth, and equipped with a zero free play gearbox (see Figure 6, right).

Figure 6: The configuration of the movable aileron (left) and the RSF-5B by Harmonic Drive to control both the aileron and the IWT.

Both control surfaces were 3D printed using the same material of aerodynamic sectors. In this case, the approach had the further benefit of embedding the required female portion of the hinging mechanisms and consequently reducing the number of parts to manufacture. To ensure sufficient stiffness of these slender elements, especially the aileron, they were enforced internally by internal ribs and this can be easily done due to the 3D printing approach adopted.

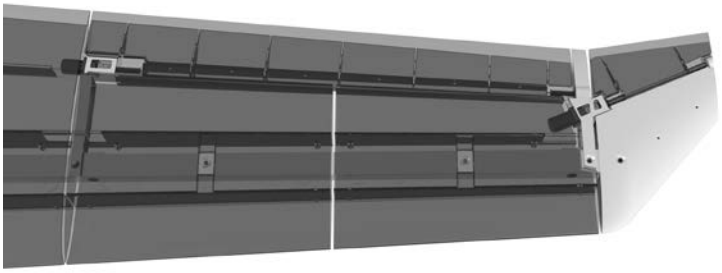

Figure 7: Overview of the IWT actuation and installation.

In terms of control approach, a PID controller based on two possible configurations, i.e. single and double loop [36], depending on the number of angular rotation sensors adopted and implementing the same saturation of the real actuator, has been designed for both aileron and IWT and its main characteristics are reported in Table 1.

Table 1. Actuator's performances.

	Single Loop	Dual Loop
Bandwidth	10 Hz	
Gain margin	12 dB @ 18 Hz	6,62 dB @ 16 H
Phase margin	66 degs @ 11 Hz	70.5 degs @ 1a Hz

D. Fuselage and Tailplanes

The main structural component of the fuselage is a composite beam of hollow square cross-section spanning from nose to tail but split into two parts connected together at the central wing root region. The beam is manufactured in composite (carbon fibre) to obtain natural frequencies well above those of the wing, minimizing couplings and undesired excitation of the system. The two halves of the beam are bolted together to a connecting aluminium insert.

The hollow square beam, seen in Figure 8, fits snugly within the composite beam and defined the bolting region for the wing support. From the perspective of fuselage skins, the outer surfaces are defined by three main components: a front fuselage section, a rear fuselage, and the fuselage nose. All of them are in composite, but their draping and thickness differ. The nose is made by a light glass fibre skin since it is used just to close the fuselage and not special loads are applied to it. The central and rear parts of the fuselage skins are made by carbon fabric reinforced by rohacell to increase the global stiffness to have the fuselage mode shapes at a well higher frequency than the ones of the wing. Ten carbon fibre ribs form the internal part of the fuselage covers. These reinforcement elements have the purpose of supporting the otherwise large external panel. In this way, the skin panels are partitioned into smaller ones and hence increasing the buckling eigenvalues.

Figure 8: External (top) and internal (bottom) view of the fuselage.

The vertical tail sub-assembly stems from the rear end of the fuselage beam. Note how it had already been cut at the appropriate angle. An aluminum beam with a rectangular section introduces the desired cone angle and is attached employing a U-shaped bracket setting in the composite beam. Upwards shoot two spars and an enforcing plate component. Together these elements define the vertical tailplane, which is subsequently crowned by the trimming mechanism (Figure 9, left). Such a mechanism is composed of a machined plate and two brackets which form the axis for the rotation of the horizontal tail. An arm also extends aft to position the elevator actuator, analogous to the already described on the wing, allowing for the cohesive rotation of both lifting and control surfaces. A spar extends outwards to assemble the horizontal tail, as shown in the following Figure 9, right.

Figure 9: Vertical tail (left) and the Htail including the trimming device and the elevator actuation systems (right).

The structural solution adopted for the horizontal tailplane is similar to the one adopted for other components, i.e. a sandwich structure made of carbon fibre skin and a Nomex core. Three hinges were embedded in the core, and all components were bolted to the skin. The hinges provide support for the elevator, which was built in the same way as the wing control surfaces by 3D printing technology. Figure 10 shows the complete model, installed on the WAS system.

Figure 10: The complete model installed on the WAS System.

E. The Weight Augmentation System (WAS)

The WTT3 wind tunnel model, representing half of the reference aircraft, is connected to the floor with dedicated support able to guarantee a free-free motion in plunge and pitch. This configuration appears challenging from the model trim point of view, due to the presence of the *1g* loads. Indeed, since the wing is in a vertical position the weight does not offer any counterbalance of the lift force. The adopted strategy required the use of a dedicated device able to produce the necessary force able to balance the lift produced at different test speeds. The name of this device is Weight Augmentation System (WAS) that was conceived and manufactured during a previous EU project named GLAMOUR [35]. It is composed of a sliding mechanism to allows for the plunge motion driven by an electrical servo-actuator controlled in force, as to be able to guarantee a constant force, corresponding to the *1g* trim loads (see Figure 11, left). Thanks to this system, it is possible to trim the model for different flight conditions so to assess the validity of the gust alleviation strategies for a large portion of the flight envelope. The hardware constituting the WAS system is covered by the so-called dummy floor over which the wind tunnel model is sliding in plunge and pitch motion.

Figure 11: The Weight Augmentation System (left) and the finalized WTT3 model inside the test room, showing the dummy floor covering the WAS (right).

VI. Numerical Modelling and Ground Vibration Test (GVT)

Different finite element models have been used during the development of the WTT3 model. Detailed models of single components have been used for design and verification purposes as well as to generate reduced order models when necessary. On the other hand, a quasi-stick model has been adopted for the numerical vs. correlation analysis during the GVT tests as well as for the aeroelastic simulation analyses (see Figure 12 and Figure 13).

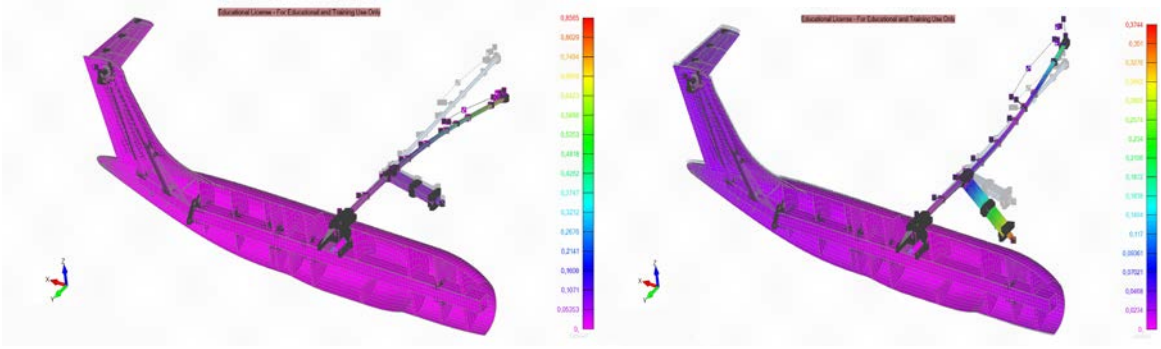

Figure 12: First out of plane bending (left) and the first torsional modes (right).

The GVT campaign was carried out having the complete model installed on the WAS system and using an electrodynamic shaker for the excitation (see Figure 14). A set of 80 accelerometers allowed to capture the relevant mode shapes. A quick updating has been applied to the quasi stick model to tune its actual behavior as to reproduce the experimental behavior.

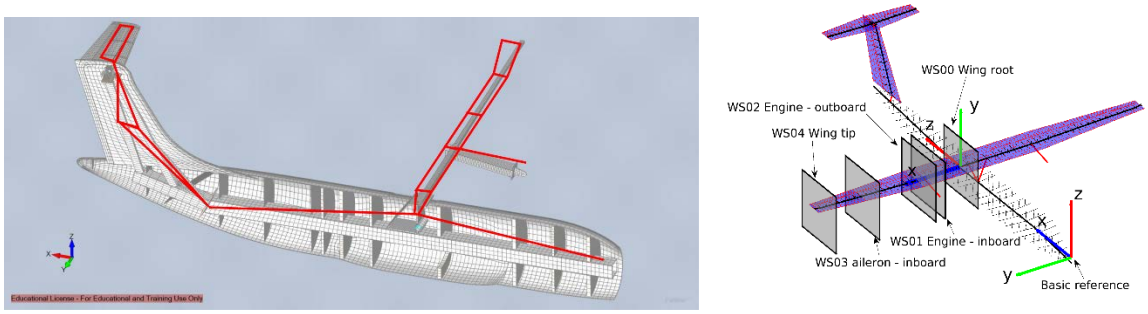

Figure 13: The experimental mesh for the GVT overlapped to the 3D FEM mesh (left) and the aeroelastic model for gust load alleviation simulations including the considered monitoring stations spanwise (right).

Figure 14: Images taken during the GVT activity.

VII. The Wind Tunnel and the Gust Generator

The GVPM is a medium-size low-speed wind tunnel highly dedicated to helicopter and airplane model testing. Due to this facility, POLIMI is a member of SATA since 2003. The wind tunnel can operate both in a closed test section and in an open jet configuration. The closed test section is 6 m long, 4 m wide and *3.84 m* high. The first *5 m* part of the closed test section is removable to allow for off-line test preparation (or, in case, to allow for open jet tests). Two interchangeable closed test sections (the ”yellow” and the ”blue” one) are available. A high flow ratio compressor supplies compressed air for the air-bearing movement systems that are used to move the closed test sections (see Figure 15) and the other heavy structures or machines.

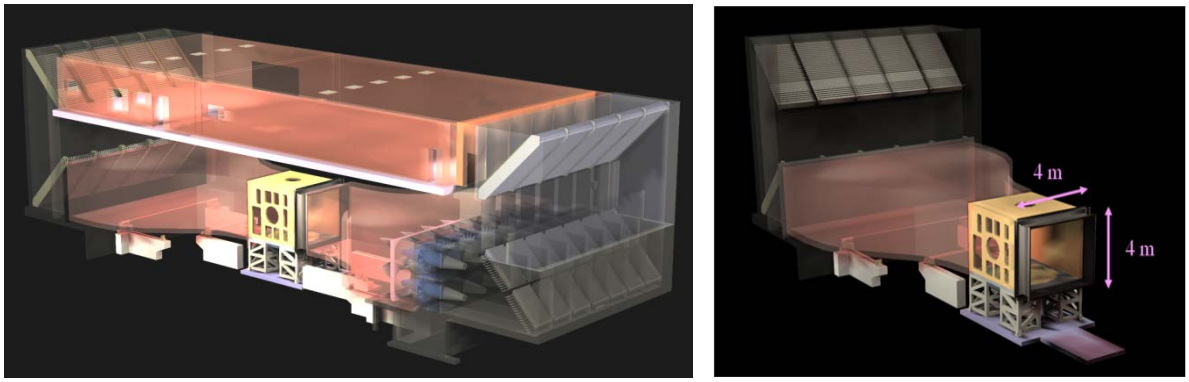

Figure 15: The POLIMI's wind tunnel.

The flow quality is adequate for aeronautical testing (the turbulence level is less than 0.1%). The airflow is produced by 14 fans with a total power of 1.4 MW. By virtue of the heat exchanger, the wind tunnel testing is not affected by any significant temperature gradient so that test duration is not limited by wind tunnel overheating. The wind tunnel is controlled in velocity (from *3 m/s* up to *55 m/s*). The maximum velocity of *55 m/s* corresponds to a maximum Mach number of *0.16* and to Reynolds number per meter of about *3.8* million. As this usually produces a model Reynolds number lower than in the full-scale aircraft, transition strips can be positioned on the model surface. Adhesive tape transition strips are used at GVPM, sized according to NASA TN-3579.

The velocity feedback for the control is obtained by dynamic pressure measurement together with the measurement of thermodynamic quantities necessary to compute the fluid density. The test condition parameters continuously monitored during the test are dynamic pressure, absolute pressure, absolute temperature, and relative humidity. Thus an accurate evaluation of the actual fluid density is possible allowing the flow velocity to be obtained from the dynamic pressure.

To perform the gust response wind tunnel test, a dedicated device to produce the typical sinusoidal or *1-cos* gust profile as requested by the CS certification rules has been designed and manufactured. Since the test will be performed in the close chamber configuration, the capability of reaching the right gust velocity and a sufficient homogeneous gust field around the model has to be evaluated in the preliminary design phase, due to the wall effect and the dissipation of the gust along the chamber. The main design parameters playing a major role in the design of the gust generator are the number of gust vanes, its chord length, and the maximum rotation angle. Indeed, different and opposite requirements have to be combined. While the increase of the chord of the gust vane could potentially increase the maximum gust generated, the increased inertia of the vanes could limit the maximum frequency reachable. More, the increased number of the vanes could increase the maximum gust obtainable but at the same time generates disturbances in the normal flow even if when the vanes are not actuated. The final configuration obtained after an optimization process is based on the use of 6 vanes of 0.4*m* chord. Any couple of vanes is connected together and actuated by a single linear electromagnetic actuator, similar to one adopted for the WAS system. A dedicated control loop allows creating a *1-cos* gust profile. The 6 vanes have been manufactured by POLIMI using a single steel square tube as the main spar, the aerodynamic shape made by styrofoam and covered by glass fiber so to minimize the inertia and maximize the available excitation bandwidth.

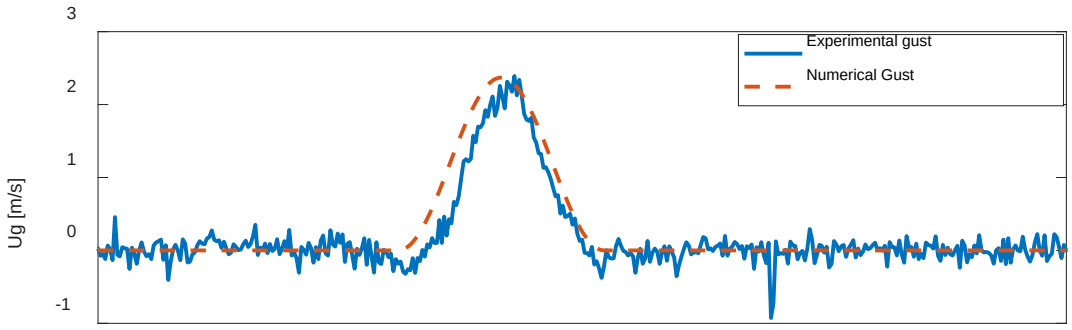

Figure 16: Comparison between ideal 1-cos gust and the one created with the gust generator

VIII. Wind Tunnel Test Results

The wind tunnel test campaign aiming at the validation of GLA systems was carried out in January and September 2021 (see Figure 16). The fight envelope *V-n* diagram of reference aircraft defines the set of flight conditions relevant for certification. The ones considered here are based on the three most relevant velocities such as the V_C the cruise velocity, V_D the dive velocity, and V_{Mo} the maximum operating velocity. Starting from these values and applying the due scaling process, the corresponding flight conditions for the wind tunnel model are the ones summarized in Table 2: the two highest velocities have been tested in wind tunnel.

Table 2: The flight conditions scaled down from the Reference Aircraft.

Flight point	Altitude [m]	EAS [m/s]	Mach
Aerodynamic design point	0	20.033	0.059
Maximum operating speed - sea level	0	**23.150**	0.068
Maximum operating speed - corner point	0	22.667	0.067
Maximum operating speed - max altitude	0	18.750	0.055
Dive speed - sea level	0	27.00	0.079
Dive speed - corner point	0	**26.290**	0.077
Dive speed - max altitude	0	21.667	0.064

EASA requires the analysis of discrete gust loads for a range of gust gradients. Once the gust amplitude is computed, the only remaining degree of freedom is the gust gradient which relates to the spatial wavelength of the *1-cos* model. To limit the number of gust condition to be tested experimentally, two gust conditions were selected, i.e. the tuned one, having the same frequency of the 1st wing bending mode, and the worst one, so the one able to produce the maximum peak of the internal load, as reported in Table 3. It must be highlighted that thanks to the WAS system, during the test both the *1g* and the gust loads are generated for each test point. Indeed, the model is at first trimmed at the selected flight point of interest, then it is impacted by the gust profile produced by the gust generator.

Table 3: The gust profile selected to be validated during the wind tunnel test campaign.

ID	Airspeed [m/s]	Amplitude [m/s]	Frequency [-]
G1	26.28	1.21	0.75
G2	26.28	-1.21	0.75
G3	26.28	1.16	1
G4	26.28	-1.16	1
G5	22.66	2.37	0.75
G6	22.66	-2.37	0.75
G7	22.66	2.26	1
G8	22.66	-2.26	1

Figure 17: The WWT3 model installed into the test chamber ready for testing.

The wind tunnel model wing is instrumented by strain gauge bridges for bending and torsion in four monitoring stations spanwise. In this view, it is very easy to evaluate the performances of different controllers and architectures in terms of alleviation capability. During the typical experimental campaign, a large amount of data is collected, since many are the parameters that can be tuned to completely evaluate the performances of the GLA controller: among the other, the sampling frequency, the active control frequency, the bandwidth of the actuators, as well the sensitivity with respect to gains and delays variations have been investigated. Table 4 summarizes the typical results of one of the configurations tested.

A. The controllers' architecture

Among the different control architectures investigated during the entire AIRGREEN2 project the following two are considered here, both of them based on SOF approach, SOF401 and SOF03. The first one, SOF401, uses all the primary control surfaces potentially available on an aircraft, i.e. ailerons and elevator plus the novel wingtip control surface. The second one, SOF003, uses only the wingtip control surfaces. The rudder is not considered yet since the focus is on the vertical gust load investigation only, justified by the adoption of a half aeroelastic model for wind tunnel validation. The first controller has been tested aiming at the evaluation of maximum alleviation capabilities using all the control surfaces available, while the second one has been tested in view of the final flight test campaign scheduled inside CS2 project and expected by the end of 2022. Indeed, during this flight campaign, only the innovative wingtip will be used. For this reason, due to the difficulties in practical flight testing of GLA controllers due to the impossibility to predict and control the gust input, the gains of SOF003 has been ad hoc tuned to guarantee also Maneuver Load Alleviation (MLA) capabilities that can be more easily validated by pilot imposed specific high g maneuvers, such as sustained turns. While in terms of outputs the two controllers differ for the number of control surfaces actuated, for what concerns the feedback channels they share the same architecture based on four measurements: vertical acceleration at the left and right wingtips, CoG vertical acceleration and pitch angular velocity. When structural velocities are requested, they are obtained by pseudo integration of the measured acceleration to avoid saturation due to possible offset signals present on the measurement channels.

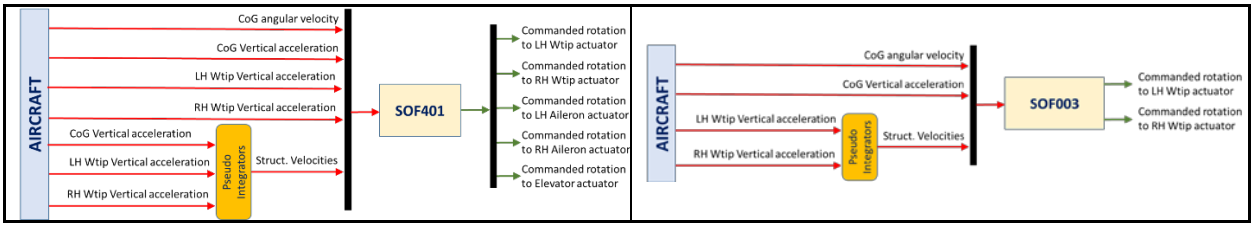

Figure 18: The SOF401 (left) and SOF003 (right) controllers, respectively.

B. Control architectures wind tunnel tested: full scale aircraft vs. WTT3

The validation of active control systems for load alleviation using wind tunnel models is heavily impacted by the scaling process adopted and by the different hardware adopted for full scale in flight test and for the wind tunnel test. Any consideration about the obtained performances during wind tunnel tests must be evaluated in light of these considerations. Aiming at this goal, simulation activity as well as the wind tunnel test campaign have been carried out to clarify these aspects by dividing the controllers in two main families: slow and fast controllers.

The **slow controllers** are mainly based on the hardware available currently for flight test activities. In particular, the performances impacting on the controllers' performances are the maximum sampling frequency, the data transfer rate, the max control frequency. These performance limitations have been introduced in the numerical simulation model to generate the reference Gain matrix corresponding to the max gain values applicable before reaching the instability of the system.

The **fast controllers** have been obtained by relaxing the limitation of the current hardware using more realistic values compatible with the technology available in the next future for new aircraft. Thanks to this hardware limitations removal, during the simulation phase it was possible to increase by a factor of 3 the gain matrix obtaining the expected load alleviation performances without incurring in any control instability.

For what concerns the controllers implemented on the WTT3 model and used for the experimental validation it is important to remind the following aspects:

- The dynamic properties of the wind tunnel model are matched by the GVT and model updating experimental sessions.

- The architecture of the controllers, including the non linearities of the actuation systems such as the saturation are exactly the ones implemented at the full scale level, are the same, thanks to the iso-frequency scaling.
- The only mismatch between the two models (WTT3 and full scale aircraft) is related to the lower effectiveness of the control surfaces in the wind tunnel model w.r.t the DLM simulations at full scale level due to low Reynolds number and presence of slots.
- Different methods are available to patch the Generalized Aerodynamic Forces matrices. In this case POLIMI performed a scaling procedure before start the wind tunnel close loop control tests.
- The structure is excited by frequency sweeps applied with the control surfaces. Then, the FrF functions, for example acceleration/rotation are computed and compared with the corresponding ones obtained by numerical simulations on full-scale aircraft. The scaling factor obtained, is used to scale up the experimental gains matrix during the close loop test.

Figure 19 shows that in the case of aileron there is a loss of effectiveness of about 25%, meaning that the corresponding gains have to be increased to produce the same results on the full-scale aircraft, or that the numerical results have to be decreased by 25% before the comparison with the experimental ones.

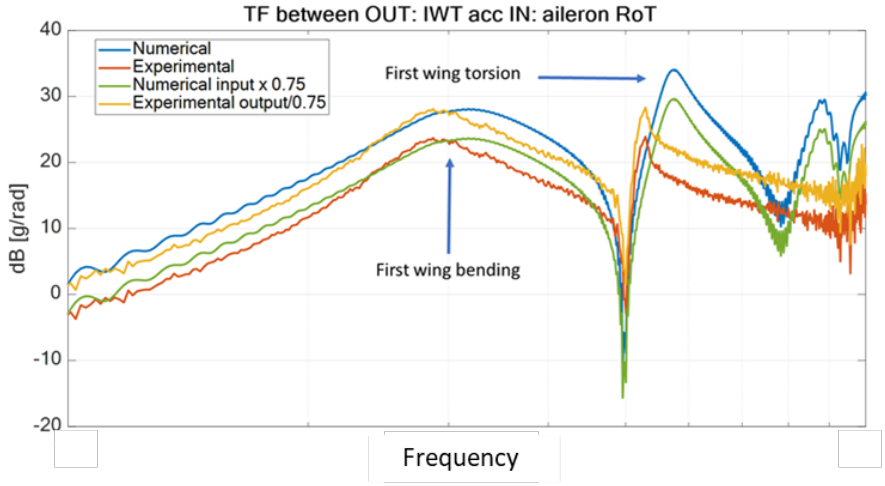

Figure 19: Typical transfer function measured in the wind tunnel by applying a frequency sweep with the aileron.

For these reasons, the gains matrix used in WTT3 fast controllers is based on the reference values of full aircraft multiplied by 4 and not by 3 like in the numerical simulations. In this way, the wind tunnel results are expected as comparable to the numerical ones at full scale aircraft level.

C. Gust Load Alleviation Capabilities Assessment

The wind tunnel test campaign generated a large amount of data concerning different controllers, values of gains, gust amplitudes (positive and negative) and frequency for two different velocities, together with many interesting response quantities, from internal loads in different location spanwise, to local accelerations and velocities. It is not easy to derive a synthetic performance index representative of all the alleviation capabilities. In the following Tab just the most representative results are reported in terms of average alleviation capability of bending moment in different monitoring stations spanwise for all the gust load conditions in case of fast controllers. In this case, fast means a frequency of 1kHz for both the control loop and the sampling frequency of all the measured quantities. The bandwidth of all the actuators is fixed to 10 Hz. It is possible to see an average alleviation, in terms of decrease of the first time response peak of about 3% in case of wingtip only and 20% in case of all control surfaces. These values are directly comparable with the numerical simulations carried out during the design phase on wind tunnel model but also on the full scale aircraft (See Figure 20 and Figure 21).

Table 4: Some preliminary wind tunnel test results in terms of bending alleviation.

Controller	Average Delta Bending WS00 [%]	Average Delta Bending WS01 [%]	Average Delta Bending WS02 [%]	Average Delta Bending WS03 [%]
SOF003 Fast	-1.95	-2.79	-3.33	-3.84
SOF401 Fast	-19.79	-22.76	-22.67	-20.07

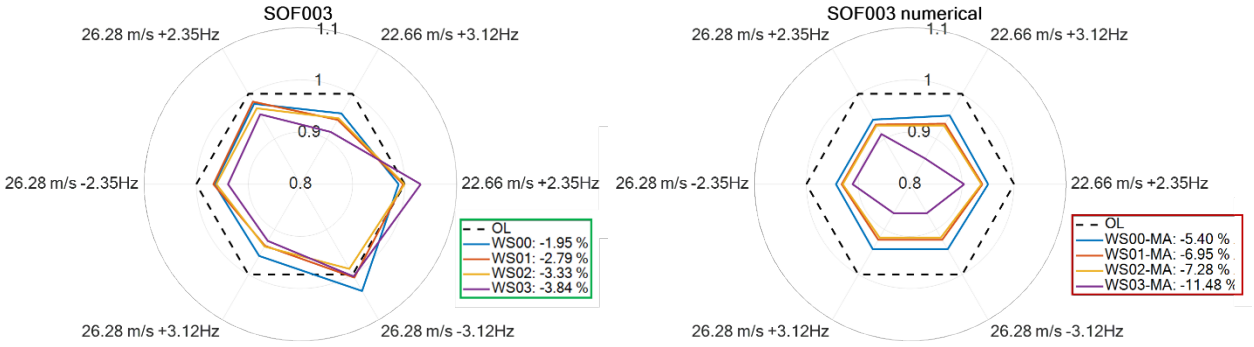

Figure 20: Load attenuation performances for SOF003 controllers: numerical vs. experimental correlation.

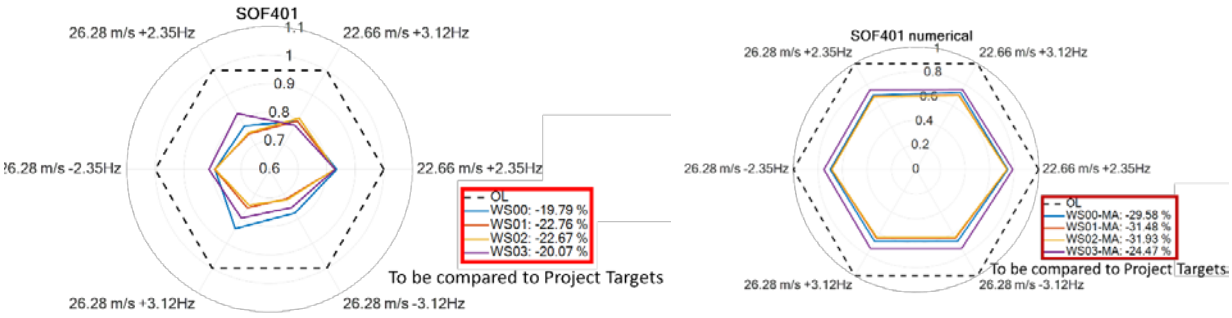

Figure 21: Load attenuation performances for SOF401 controllers: numerical vs. experimental correlation.

IX. Conclusions

The paper summarizes the structure and goals of the EU-CS2-AIRGREEN2 project with a special emphasis on the activity regarding the Gust Load Alleviation technologies. The WTT3 large scale aeroelastic model is then introduced and details concerning the scaling strategy, the structural configuration as well the actuation systems, and the wind tunnel setup are also provided. Finally, the results of an extended wind tunnel test campaign are discussed and assessed.

The experimental campaign has been successfully completed at POLIMI's Large Wind Tunnel without relevant issues, despite the complexity of the setup involved. For what concerns the results, in comparison with the expected alleviation capabilities based on numerical simulations based on full scale aircraft, the following conclusions can be drawn, divided by test category. For what concerns the result of the slow controller, it is possible to say the following. In some cases, it is difficult to find a clear correlation among the test results: sometimes the controller alleviates more than the numeric, in other it is the opposite; mean alleviation obtained by numerical simulation and experimental results is comparable. For what concerns the results for fast controllers it is possible make the following comments: the accuracy and repeatability of the experimental results are quite better, thanks to the increased gains adopted; mean alleviation obtained by numerical simulation and experimental results is comparable and in the case of SOF401 (full set of control surfaces) are in line with the expected project targets (19% reduction of Root Bending Moment).

On the basis of the reported conclusions it is possible to summarizes the lessons learned together with few suggests for next steps of this research.
In the setup adopted for wind tunnel testing still appear some sources of unknowns that generate a level of non-repeatability not negligible. One of them is related to the presence of friction. Despite this aspect has been fully investigated and some specific solutions to minimize this effect included in the control software driving the WAS, this aspect is still present.
The main challenge in the design of an aeroelastic wind tunnel model is to accurately capture the aeroeastic behavior of the full scale aircraft. However, in a hybrid model such as the WTT3, where the wing is actually elastic while the fuselage is not, and due to the complex hardware included into the model, it is really hard to keep all the quantities properly scaled. In general, the mass properties of the entire model are higher than the correct scaled values. Unfortunately, this effect, coupled with the previous one related to the friction, could produce a rigid motion different from the one in the reality, impacting from the control point of view on the gains related to the rigid motion states, such as the ones representing the CoG motion, so decreasing the effectiveness of the active control low in general. For this reason, POLIMI is now implementing a dedicated 'Flight Control System' able to trim the model automatically and able to use the WAS not only for trimming but also to drive the model so to produce the right rigid motion response.
The wind tunnel is a noise environment due to the flow generators, the gust generator actuators as well the WS actuator itself. During the test with low control gains and/or low excitation level the risk is that the variation of some structural responses can generate low level signals of the same order of magnitude of background noise.
The impact of hardware performances is relevant, making the alleviation target achievable or not. Indeed, low sampling rate and frequency control or data transfer prevent to increase the control gains and introduce phase delay able to generate instabilities.
To conclude, it is expected that the load alleviation performances measured during the wind tunnel test are slightly underestimated with respect the actual results that can be obtained at the full aircraft level.

X. Acknowledgements

The AirGreen2 Project has received funding from the Clean Sky 2 Joint Undertaking, under the European's Union Horizon 2020 research and innovation Programme, under grant agreement No. 807089.

XI. Disclaimer

The present work reflects only the authors' view and the European Commission and Clean Sky 2 JU are not responsible for any use that may be made of the information contained in this paper.

XII. References

[1] Work programme 2013 Cooperation Theme 7 Transport (including Aeronautics), European Commission C (2012) 4536 of 9 July 2012.
[2] European Aeronautics: A Vision for 2020. Group of Personalities. 2001, ISBN 92-894-0559-7.
[3] ACARE Strategic, Research and Innovation Agenda Vol. 1, Realising Europe's Vision for Aviation, September 2012.
[4] Burris, P. M. and Bender, M. A., "Aircraft Load Alleviation and Mode Stabilization (LAMS): B-52 System Analysis, Synthesis, and Design," Tech. rep., Air Force Flight Dynamics Laboratory. Air Force Systems Command. Wright-Patterson Air Force Base, Ohio, 1969.
[5] Regan, C. D. and Jutte, C. V., "Survey of Applications of Active Control Technology for Gust Alleviation and New Challenges for Lighter-weight Aircraft," Tech. rep., NASA, TM–2012-216008, 2012.
[6] Britt, R. T., Volk, J. A., Dreim, D. R., and Applewhite, K. A., "Aeroservoelastic Characteristics of the B-2 Bomber and Implications for Future Large Aircraft," Tech. rep., DTIC Document, 2000.
[7] Hahn, K.-U. and Schwarz, C., "Alleviation of atmospheric flow disturbance effects on aircraft response," 26th Congress of the International Council of the Aeronautical Sciences (ICAS), Anchorage, Alaska, USA (September 2008), 2008.

[8] Matsuzaki, Y., Ueda, T., Miyazawa, T., and Matsushita, H., "Wind tunnel test and analysis on gust load alleviation of a transport-type wing," 87-0781. 28th Structures, Structural Dynamics and Materials Conference, 1987.
[9] Kuzmina, S. I., Ishmuratov, F., Zichenkov, M., and Chedrik, V., "Integrated numerical and experimental investigations of the Active/Passive Aeroelastic concepts on the European Research Aeroelastic Model (EuRAM)," Journal of Aeroelasticity and Structural Dynamics, Vol. 2, No. 2, 2011, pp. 31–51.
[10] Karpel, M., Moulin, B., Feldgum, V., et al., "Active alleviation of gust loads using special control surfaces," 47th AIAA/ASME/ASCE/AHS/ASC Structures, Structural Dynamics, and Materials Conference, 1-4 May 2006, Newport, Rhode Island, Vol. AIAA 2006-1833, 2006.
[11] Moulin, B. and Karpel, M., "Gust loads alleviation using special control surfaces," Journal of Aircraft, Vol. 44, No. 1, 2007, pp. 17–25.
[12] Wu, Z., Chen, L., and Yang, C., "Study on gust alleviation control and wind tunnel test," Science China Technological Sciences, Vol. 56, No. 3, 2013, pp. 762–771.
[13] N.Nguyen, Flight Control of Flexible Aircraft, NESC GNC Meeting at NASA ARC, January 25, 2017
[14] Tollmien, W., Schlichting, H., G¨ortler, H., and Riegels, F., "Uber Tragfl¨ugel kleinsten induzierten Widerstandes," ¨ Ludwig Prandtl Gesammelte Abhandlungen, Springer, 1961, pp. 556–561.
[15] Jones, R. T., "The spanwise distribution of lift for minimum induced drag of wings having a given lift and a given bending moment," Tech. rep., NACA, Tn–2249, 1950.
[16] Whitcomb, R. T., "A design approach and selected wind tunnel results at high subsonic speeds for wing-tip mounted winglets," Tech. rep., NASA, TN D-8260, 1976.
[17] Ning, A. and Kroo, I., "Multidisciplinary considerations in the design of wings and wing tip devices," Journal of Aircraft, Vol. 47, No. 2, 2010, pp. 534–543.
[18] Sensburg, O., Becker, J., Lusebrink, H., and Weiss, F., "Gust Load Alleviation on Airbus A 300," ICAS-82-2.1.1, 1982.
[19] Ricci, S., Castellani, M., and Romanelli, G., "Multi-fidelity design of aeroelastic wing tip devices," Proceedings of the Institution of Mechanical Engineers, Part G: Journal of Aerospace Engineering, Vol. 227, No. 10, 2013, pp. 1596–1607.
[20] Castrichini, A., Siddaramaiah, V. H., Calderon, D., Cooper, J. E., Wilson, T., and Lemmens, Y., "Nonlinear Folding Wing Tips for Gust Loads Alleviation," Journal of Aircraft, Vol. 53, No. 5, 2016, pp. 1391–1399.
[21] Castrichini, A., Cooper, J. E., Wilson, T., Carrella, A., and Lemmens, Y., "Nonlinear Negative Stiffness Wingtip Spring Device for Gust Loads Alleviation," Journal of Aircraft, Vol. 54, No. 2, 2017, pp. 627–641.
[22] 19Cheung, R., Castrichini, A., Rezgui, D., Cooper, J., and Wilson, T., "Testing of Wing-Tip Spring Device for Gust Loads Alleviation," 58th AIAA/ASCE/AHS/ASC Structures, Structural Dynamics, and Materials Conference. 9 - 13 January 2017, Grapevine, Texas, Vol. 1317, 2014.
[23] 20Chekkal, I., Cheung, R., Wales, C., Cooper, J. E., Allen, N., Lawson, S., Peace, A. J., Hancock, S., Cook, R., Standen, P., and Carossa, G. M., "Design of a morphing wing tip," Proceedings of the AIAA SciTech 22nd AIAA/ASME/AHS Adaptive Structures Conference, National Harbor, MD, USA, Vol. 1317, 2014.
[24] Cooper, J. E., Chekkal, I., Cheung, R. C. M., Wales, C., Allen, N. J., Lawson, S., Peace, A. J., Cook, R., Standen, P., Hancock, S. D., and Carossa, G. M., "Design of a Morphing Wingtip," Journal of Aircraft, Vol. 52, No. 5, Jul 2015, pp. 1394–1403.
[25] Vasista, S., Riemenschneider, J., Van de Kamp, B., Monner, H. P., Cheung, R. C., Wales, C., and Cooper, J. E., "Evaluation of a Compliant Droop-Nose Morphing Wing Tip via Experimental Tests," Journal of Aircraft, Vol. 54, No. 2, 2016, pp. 519–534.
[26] 23Heinen, C., Wildschek, A., and Herring, M., "Design of a winglet control device for active load alleviation," International forum on aeroelasticity and structural dynamics, Bristol, UK , 2013, pp. 24–26.
[27] Wildschek, A., Prananta, B., Kanakis, T., Tongeren, H., and Huls, R., "Concurrent optimization of a feed-forward gust loads controller and minimization of wing box structural mass on an aircraft with active winglets," 16th AIAA/ISSMO multidisciplinary analysis and optimization conference, Dallas, TX , 2015, pp. 22–26. 17 of 18 American Institute of Aeronautics and Astronautics Downloaded by POLITECNICO DI MILANO on January 26, 2018 | http://arc.aiaa.org | DOI: 10.2514/6.2018-1442.
[28] Johnston, J. F., "Accelerated development and flight evaluation of active controls concepts for subsonic transport aircraft. Volume 1: Load alleviation/extended span development and flight tests," Tech. rep., NASA-CR-159097, September 1979.
[29] Bernelli-Zazzera, F., Mantegazza, P., Mazzoni, G., and Rendina, M., "Active Flutter Suppression Using Recurrent Neural Networks," Journal of Guidance, Control, and Dynamics, Vol. 23, No. 6, 2000, pp. 1030–1036.

[30] Thornton, S. V., "Reduction of structural loads using maneuver load control on the Advanced Fighter Technology Integration (AFTI)/F-111 mission adaptive wing," Tech. rep., NASA, TM-4526, 1993.
[31] Giesseler, H.-G. and Beuck, G., "Design procedure for an active load alleviation system (LAS) for a modern transport aircraft," Congress of the International Council of the Aeronautical Sciences (ICAS), Toulouse, Fr (1984), 1984.
[32] 30Company, B. C. A., "Integrated Application of Active Control (IAAC) Technology to an advanced subsonic transport project — Final Act Configuration Evaluation," Tech. rep., NASA, CR–3545, 1982.
[33] Syrmos, V. L., Abdallah, C. T., Dorato, P., and Grigoriadis, K., "Static Output Feedback — A Survey," Automatica, Vol. 33, No. 2, 1997, pp. 125–137.
[34] Fonte, F., Ricci, S., and Mantegazza, P.,Gust Load Alleviation for a Regional Aircraft Through a Static Output Feedback, *Journal of Aircraft*, Vol. 52, No. 5, 2015, pp. 1559-1574.
[35] S. Ricci, A. De Gaspari, L. Riccobene, and F. Fonte, "Design and wind tunnel test validation of gust load alleviation systems," in 58th AIAA/ASCE/AHS/ASC Structures, Structural Dynamics, and Materials Conference, Grapevine, TX, USA, January 2017.
[36] A. De Gaspari, A. Mannarino, P. Mantegazza, A Dual Loop Strategy for the Design of a Control Surface Actuation System with Nonlinear Limitations, Mechanical Systems and Signal Processing, Vol. 90, 2017, p. 334-349 doi:10.1016/j.ymssp.2016.12.037.